



Scholars Research Library

Der Pharma Chemica, 2015, 7(6):287-298
(<http://derpharmachemica.com/archive.html>)



ISSN 0975-413X
CODEN (USA): PCHHAX

Antibacterial activity studies on anisotropic grown ZnO nanostructures prepared via mild experimental conditions

J. Jayashainy^a, Shibu Joseph^a, D. Muthu Gnana Theresa Nathan^a,
T. Manovah David^b and P. Sagayaraj^{a*}

^aDepartment of Physics, Loyola College, Chennai, India

^bDepartment of Chemistry, Madras Christian College, Chennai, India

ABSTRACT

Low temperature synthesis of one-dimensional (1D) zinc oxide (ZnO) under different experimental conditions is presented. The anisotropic growth characteristics of nanostructures aided by cetyltrimethyl ammonium bromide (CTAB) and hydrazine hydrate as the surfactant and reducing agent, respectively, under low temperature are investigated. The size and shape dependent structural properties of as-prepared 1D structures of ZnO are characterized using X-ray diffraction and electron microscopic techniques. Rod-like ZnO nanoparticles with significant control over the size and shape anisotropy has been observed with distinct surface morphologies. The width and length of the nanorods were significantly controlled while preserving the morphology of the nanocrystallites. Aspect ratio as high as 10 has been obtained for ZnO nanostructures assisted by CTAB and hydrazine hydrate, with excellent shape anisotropy facilitated by low temperature growth conditions. The analysis of optical-phonon peak shifts in ZnO nanorods using Raman scattering was performed to investigate the structural composition of nanorods. Adsorption and desorption isotherms are recorded to investigate specific-surface area of the ZnO nanopowders. The thermal stability and the residual chemical species of the samples are investigated by thermogravimetric analysis (TGA). The antimicrobial activity of synthesized ZnO nanostructures against Gram positive and negative bacterium is evaluated.

Keywords: Nanostructured materials; Semiconductors; Low temperature methods; Anisotropy; Electron microscopy.

INTRODUCTION

ZnO is one of the few important multifunctional semiconducting materials widely investigated for its multitude applications like energy conversion, catalysis, sensors and antimicrobial agent owing to their low-cost, non-toxicity and environment friendly properties [1-5]. It is also identified as a potential material for optical and electronic device applications due to its wide direct band gap (3.37 eV) and large exciton binding energy of 60 meV [6]. Decades of research on ZnO has resulted in the emergence of novel methods and techniques to produce 0D, 1D and 2D architectures depending on the type of applications. Fueled by the developments of innovative synthesis procedures 1D nanostructures of ZnO, like nanorods and nanowires have been identified as the potential class of material system for the future applications. Low temperature solution based synthesis of 1D metal oxide

nanostuctures has become a promising approach instead of the complex and high temperature methods and widely appreciated in terms of material quality, impurities, yield and cost.

Recently, solution grown zinc oxide nanowire arrays have been exploited in dye-sensitized solar cells (DSSCs) as an efficient photoanode alternative to traditional TiO₂ nanoparticle films [7, 8]. A significant improvement in the DSSC power conversion efficiency using branched nanowire structure of ZnO is due to a greatly augmented surface area. Wang et al. have developed a hydrothermal route on a Si wafer sputtered with a thin ZnO film for the growth of vertical ZnO nanorod arrays which exhibited enhanced sensitivity towards NH₃ gas [9]. Recent experiments demonstrate that a greater proportion of exposed polar surface on ZnO crystals leads to a greater photocatalytic activity [10, 11]. There are reports on the anti-microbial activities of ZnO, which are correlated to many factors including size, high surface area, aspect ratio and surface defects of the nanocrystallites [12, 13].

The use of ZnO thin film as seed layer is one of the promising approaches reported for wire-like nanostructure growth at low temperatures [14]. Hydrothermal is a proven low temperature approach for the preparation of 1D ZnO nanostructures due to the convenience and simplicity in fabrication [15]. Conventionally, hydrothermal process involves KOH, NaOH and NH₄OH aqueous solutions as mineralizers for the growth of ZnO nanorods. The nanorods obtained from these volatile solutions are heterogeneous in size and morphology that may not be suitable for practical applications. Less toxic and non-volatile reagents like hydrazine hydrate is considered an alternate choice to the conventional hydroxide solutions. Solochemical processing is yet another low temperature approach to prepare 1D oxide nanostructures in scalable quantities [16]. In addition, the use of surfactants offer control over nucleation and growth kinetics of nanoparticles resulting in hierarchy of 1D nanostructures. The surface defects and multi facets, the inherent properties of nanorods prepared using solution based methods is an advantage to investigate the fundamental aspects of 1D ZnO nanostructures.

In this report, some feasible low temperature approaches like hydrothermal and solochemical routes were employed to synthesis anisotropic ZnO nanostructures with high-aspect-ratios. Nanorod growth characteristics under hydrothermal condition involving CTAB and hydrazine hydrate are investigated. In addition, rod-like ZnO structures are also grown using solochemical method. Nanorod samples were systematically characterized to investigate the structural, optical and thermal properties. Antibacterial response for selected Gram positive and negative bacterium is also investigated.

MATERIALS AND METHODS

2.1 Chemicals

Zn(NO₃)₂.6H₂O, ZnCl₂, NaOH and C₁₇H₃₈BrN were purchased from Merck Specialities Pvt. Ltd., Mumbai and H₆N₂O was purchased from Avra synthesis Pvt. Ltd., Hyderabad and used as received without further purification.

The following Gram positive bacteria: *S. aureus*, *M. lutes*, *B. subtilis* and *S. epidermis*; and Gram negative bacteria: *K. pneumonia*, *E. aerogens*, *V. parahaemolyticus* and *P. aeruginosa* were used for the antimicrobial investigation. The bacterial cultures were obtained from the Institute of Microbial Technology (IMTECH), Chandigarh, India.

2.2 Synthesis of ZnO nanocrystals

CTAB assisted hydrothermal process: In a typical synthesis procedure, 0.183 g of CTAB and 4.81 g of sodium hydroxide (NaOH) were dissolved in 50 ml of distilled water to form a transparent solution (A) under mild stirring. In another beaker, 5.95 g of zinc nitrate hexahydrate (Zn(NO₃)₂.6H₂O) was dissolved in 50 ml of distilled water to form a yet another transparent solution (B). Solution A was cooled in ice-water for about 15 minutes and then mixed with solution B under vigorous stirring to form 100 ml of transparent solution. The resulting mixture was stirred for about 1 h and then transferred into a 150 ml Teflon-lined autoclave and then heated at 90° C for 5 h. The final white product was collected by centrifugation and washed with distilled water and dried at 60° C in air for 3 h.

Hydrazine hydrate assisted hydrothermal process: Initially, 0.87 g of ZnCl₂ was dissolved in 160 ml of distilled water and then 0.64 g of N₂H₄.H₂O was added into the above solution to form a slurry white precipitate. After about 1 h of magnetic stirring, the solution was transferred into a 200 ml Teflon-lined stainless steel autoclave. The autoclave was maintained at 150 °C for 8 h and then cooled down naturally to room temperature. The final white product was centrifuged and washed with distilled water and ethanol several times, and dried at 60° C in air.

Low temperature solochemical method: A jacketed three-neck glass reactor fitted with a thermometer, a condenser and an addition flask was used for the synthesis experiment. In a typical procedure, 1 g of sodium hydroxide (NaOH) was dissolved using distilled water and heated at 75 °C in the three neck flask under continuous stirring. Meanwhile, 3.71 g of zinc nitrate hexahydrate ($\text{Zn}(\text{NO}_3)_2 \cdot 6\text{H}_2\text{O}$) was dissolved in 25 ml of distilled water at room temperature and it was taken in the addition flask. The precursor solution was added drop by drop into the reactor for 1 h under vigorous stirring such that the dripping does not considerably change the temperature of the mixture. The addition of precursor solution into the alkaline solution resulted in the occurrence of precipitation immediately. The change in color of the precipitate from its initial transparent color to white color could be observed, indicating the formation of ZnO nanocrystals. After dripping, the resulting white precipitate was centrifuged followed by washing with distilled water several times and finally dried at 60 °C for 5 h.

2.3 Evaluation of antimicrobial activity

Antimicrobial activity of the as-synthesized 1D rod-like ZnO nanostructures was examined against the four Gram positive and four Gram negative bacteria by disc diffusion method. Prior to the experiment, well cleaned Petri plates were filled with 20 ml of Muller Hinton agar medium and allowed to solidify. A colony of bacteria was cultivated to ensure the confluent growth of the organism, the standard inoculums suspension was swabbed over the surface of the media using sterile cotton swab. The plates were then allowed to dry for 5 min. Subsequently, the discs with concentration of 2.5 mg/disc were placed on the surface of the plate with sterile forceps and gently pressed to ensure contact with the inoculated agar surface and left for about 30 min at room temperature for particles diffusion. Negative control was prepared using respective solvent (DMSO). Streptomycin (25µg/disc) was used as positive control. The plates were incubated for a period of 12 h at room temperature and zone of inhibition were recorded for each samples. The measure of antimicrobial activity was studied statistically from the average values obtained from the measured inhibition zone area values.

2.4 Characterization techniques

The X-ray diffraction patterns of the as-prepared nanoparticles were recorded by a GE-XRD 3003 TT using the monochromatic nickel filtered CuK_α ($\lambda=1.5406 \text{ \AA}$) radiation. Field Emission Scanning Electron Microscope (FESEM) was employed for morphological study using a CARL ZEISS SUPRA 55 which could be operated at an accelerating voltage of 20 kV. The apparatus is also attached with Energy Dispersive X-ray analyzer (EDAX). High resolution transmission electron microscopy (HRTEM) images were recorded on a JOEL JEM 2100 advanced HRTEM with an accelerating voltage of 200 kV. FT-Raman spectra of the samples were recorded using the BRUKER RFS instrument in the spectral range of 50-4000 cm^{-1} with Nd:YAG as laser source having laser wavelength of 1064 nm. Shimadzu IRAFFINITY-1 was employed for recording the FT-IR spectrum. Brunauer-Emmett-Teller (BET) surface area was measured by employing a MICROMERITICS ASAP 2020 porosimeter. Thermogravimetric (TG) and Differential Thermogravimetric Analysis (DTA) for air-dried samples were performed on a TGA7 (Perkin Elmer), under nitrogen atmosphere.

RESULTS AND DISCUSSION

3.1 X-ray diffraction study

Figure 1(a, b & c) displays the XRD patterns of the samples prepared via three different conditions. All the three diffraction peaks matched well with the bulk ZnO crystal, and conveniently indexed to the hexagonal wurtzite structure of ZnO ($P6_3mc$, $a = 3.35 \text{ \AA}$, $c = 5.21 \text{ \AA}$, JCPDS No 89-7102). The results indicate that the degree of orientation along the c -axis is altered for the hydrazine hydrate assisted ZnO sample (Figure 1b) when compared with the other samples. This is clearly evident from the intense and reduced full-width at half maximum (FWHM) of (100), (002) and (101) diffraction peaks. No crystalline impurity peak corresponding to hydroxide phase can be observed. It is clear that in all three cases, samples retained phase purity and good crystalline quality even though the experiments were performed at lower temperatures.

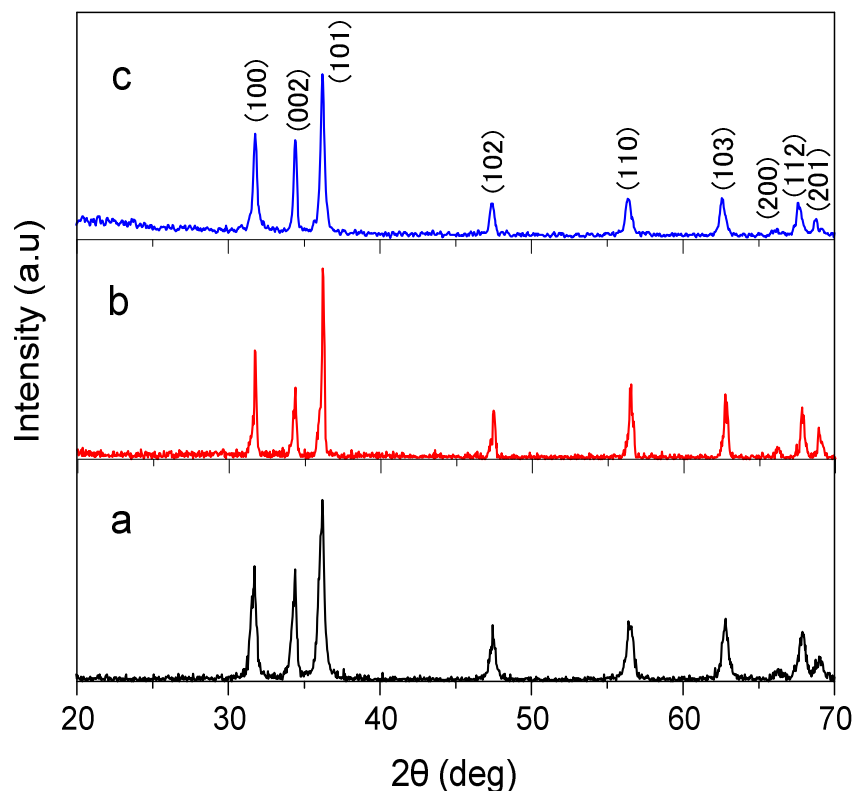


Figure 1: XRD patterns of ZnO nanorods prepared using (a) CTAB (b) hydrazine hydrate and (c) solochemical method

3.2 FESEM and EDX analysis

The typical microscopic investigation using FESEM (Figure 2a-f) depicts the growth behaviour and morphology of ZnO samples. It is clear from images that the morphology of nanocrystallites is rod-shaped which might have been facilitated by both lower reaction temperatures and the employed surfactant. It is noticeable that even in the absence of growth directing ligands, the nanorod formation (Figure 2 c-f) has not been inhibited. Thus, it is believed that the temperature plays a critical role in favouring the anisotropic growth, after the rapid nucleation. For CTAB assisted synthesis, the individual nanorods of small size were self assembled into clusters, wherein, the nanorods with average length and the width in the range 250 – 650 nm and 50 – 100 nm, respectively are assembled into bundles. The nanorods formed in the presence of reducing agent (hydrazine hydrate) are highly homogenous in size and shape (Figure 2c, d). The length of the nanorods in the range 180 and 500 nm and the width between 30 and 60 nm ascertain the fact that size of the nanorods are significantly reduced when compared to CTAB assisted growth condition and the degree of shape controlling effects are well preserved during anisotropic growth. Whereas, ZnO sample synthesized with solochemical processing (Figure 2e, f) retained the final rod-like shape of the crystallites same as other experimental conditions but with different nucleation kinetics. The finely controlled nanocrystals of spherical shape formed into nanorod-like shape may be due to the process of oriented attachment of the fine nanoparticles. The size distribution with length and the width lie in the range 300 – 550 nm and 40 – 150 nm, respectively. The aspect ratio was found to be around 9, 10 and 7 for the ZnO nanorods prepared with CTAB, hydrazine hydrate and by solochemical technique, respectively. The EDX results in Figure 3a-c, demonstrate that ZnO products contain only Zn and O and no trace of impurities are observed. It is also to be noted that oxygen atomic composition are relatively high for hydrothermal processed ZnO than the product obtained via solochemical method.

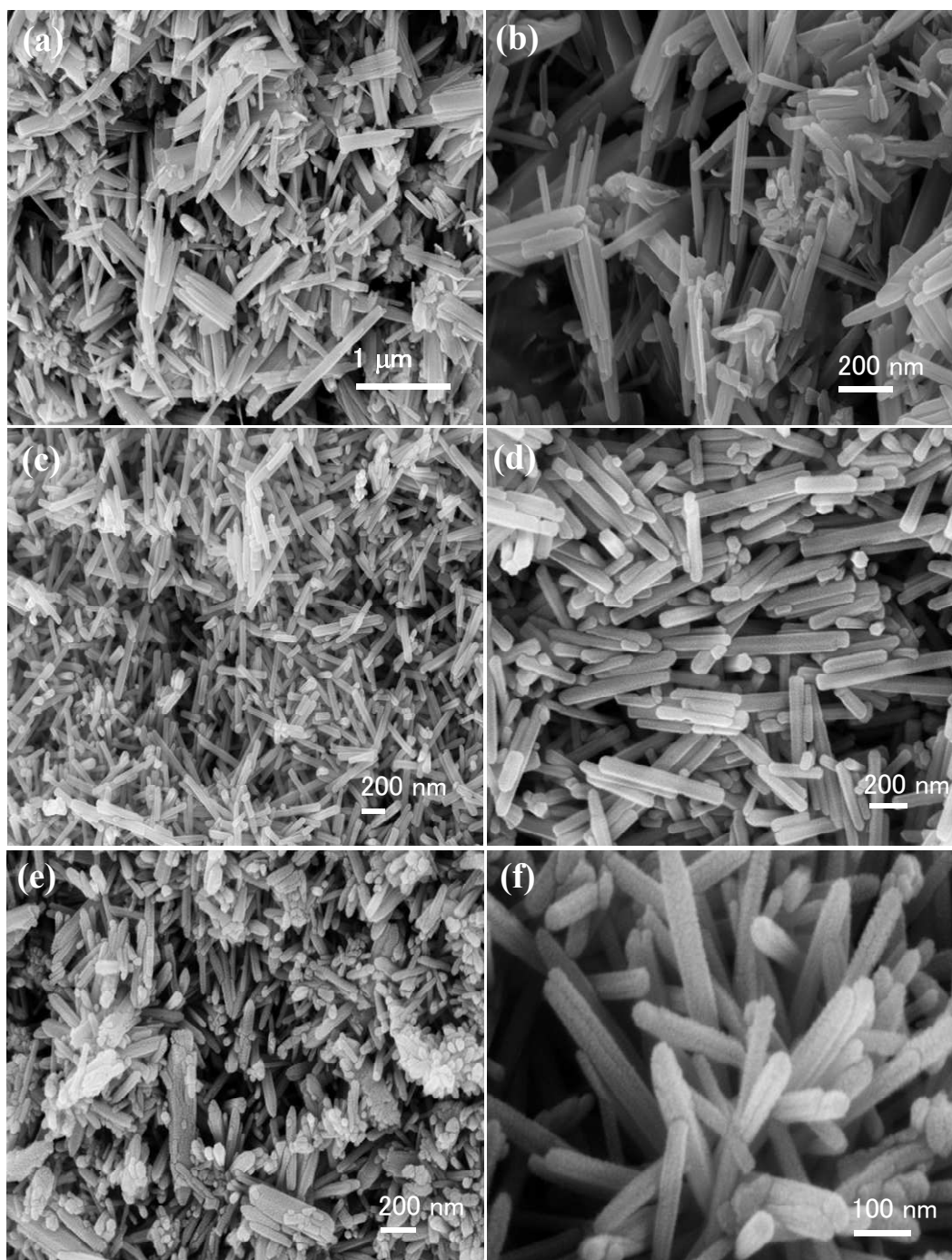


Figure 2: FESEM images of ZnO nanorods prepared using (a, b) CTAB, (c, d) hydrazine hydrate and (e, f) solochemical method

3.3 HRTEM analysis

Further structural information on ZnO nanopowders were obtained through TEM investigation. The low temperature synthesized ZnO nanorods (Figure 4a-f) reveal that the samples in general exhibit clear and distinct rod-like morphology. For CTAB assisted synthesis, smaller crystallites are formed into clusters which are less visible than the self aligned individual nanorods. The smallest size rod has 259.9 nm in length and 26.2 nm in width, which is also supported by the SEM analysis. It is widely reported that when CTAB is used in hydrothermal process, in

general it leads to flower-like nanorod bundles consisting of sword-like nanorods [17, 18]. It is worth to note here, 3D like nanorod structures is readily suppressed in the presence of CTAB. On the other hand, Figure 4c, d illustrates that the hydrazine hydrate assisted nanorods are self assembled and highly homogenous in shape and width. It is being reported that NaOH as reducing agent leads to irregular ZnO nanoparticles under the same conditions adopted for hydrazine hydrate [19]. Hydrazine hydrate as the reducing agent for nanorod synthesis is desirable for large scale synthesis of 1D ZnO with good crystallinity and shape uniformity with temperature as low as 120°C. In the case of solochemical process (Figure 4e, f), the growth is dominated by rod-like crystallite clusters which are neither aligned nor dispersed. The effect of NaOH used in solochemical synthesis is that the ratio of Zn^{2+}/OH^- is low compared to the reported value of 1:25. As a result, aggregates of rods of irregular radial structures are obtained though the nanocrystallites are highly crystalline as evidenced by the SAED pattern (inset of Figure 4e).

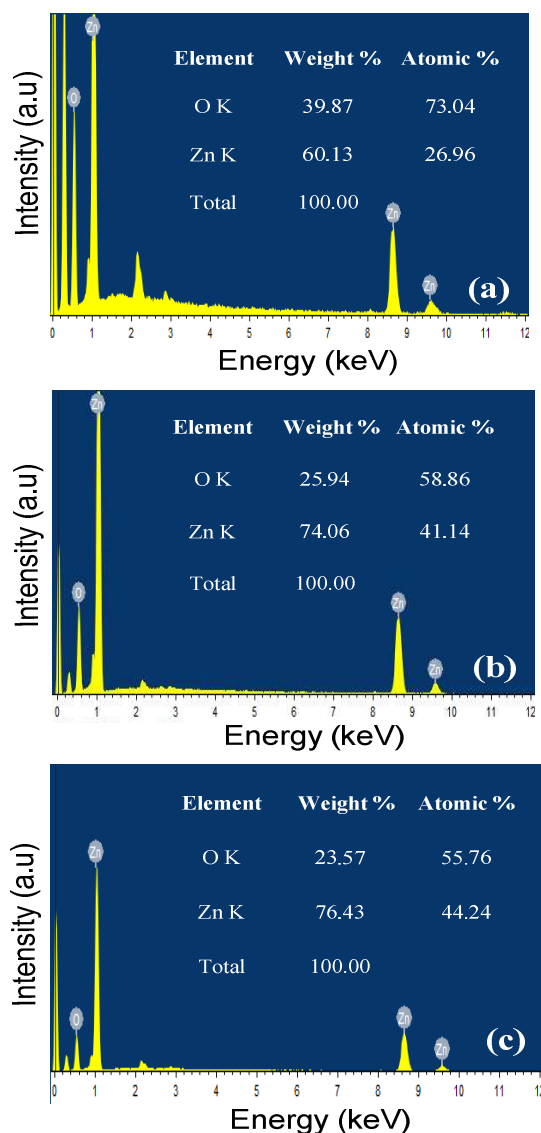


Figure 3: Energy Dispersive X-ray spectra of ZnO nanorod samples with (a) CTAB (b) hydrazine hydrate and (c) solochemical method, respectively

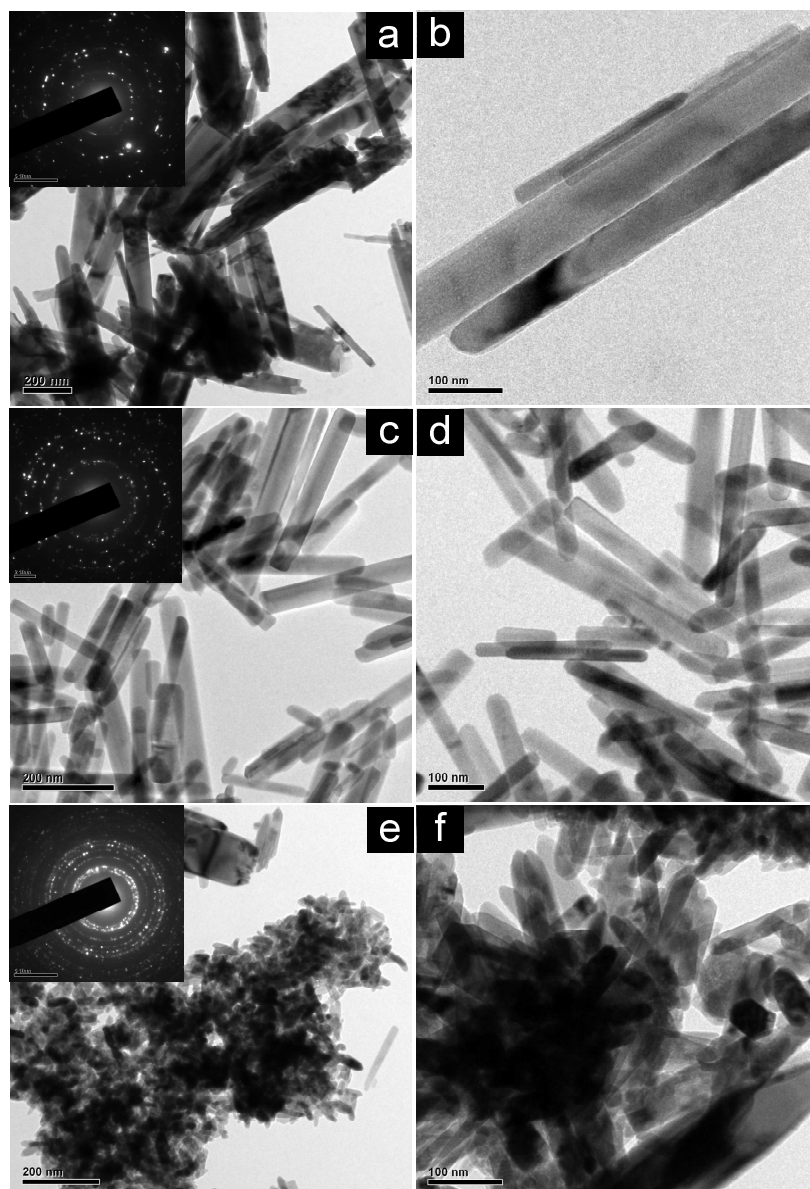


Figure 4: HRTEM images of ZnO nanorods prepared using (a, b) CTAB, (c, d) hydrazine hydrate and (e, f) solochemical method

3.4 UV-Vis Absorption Spectroscopy

The size and shape dependent optical properties of the ZnO nanorod samples were investigated by the UV-visible absorption spectra. The absorption spectra (Figure 5) consist of distinct and strong absorption peaks at 372 and 368 nm for CTAB and hydrazine hydrate assisted ZnO nanorod samples. Generally, an excitonic absorption peak appears if the defect density is considerably low [20]. Therefore, it is clear that the ZnO nanorods formed via low temperature methods are of high quality. For the solochemical processed sample, in addition to the absorption peak in the far UV region at 293 nm, a prominent peak at 665 nm is also observed. The optical absorption in the UV region may be interpreted as the characteristics of small sized nanoparticles constituting small nanorods. The optical band gap (E_g) corresponding to the absorption peaks are calculated to be 3.33 and 3.37 eV for the CTAB and hydrazine hydrate assisted hydrothermally processed samples, while the energy gap for the nanorods obtained from solochemical processing is 3.32 eV.

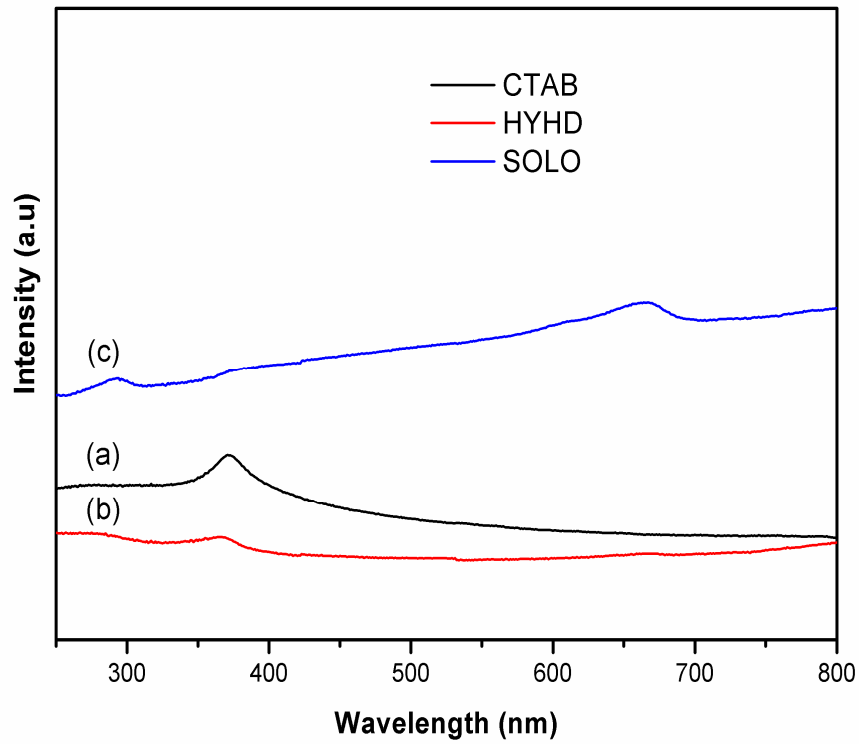


Figure 5: UV absorption spectra of ZnO nanorods prepared using (a) CTAB (b) hydrazine hydrate and (c) solochemical method

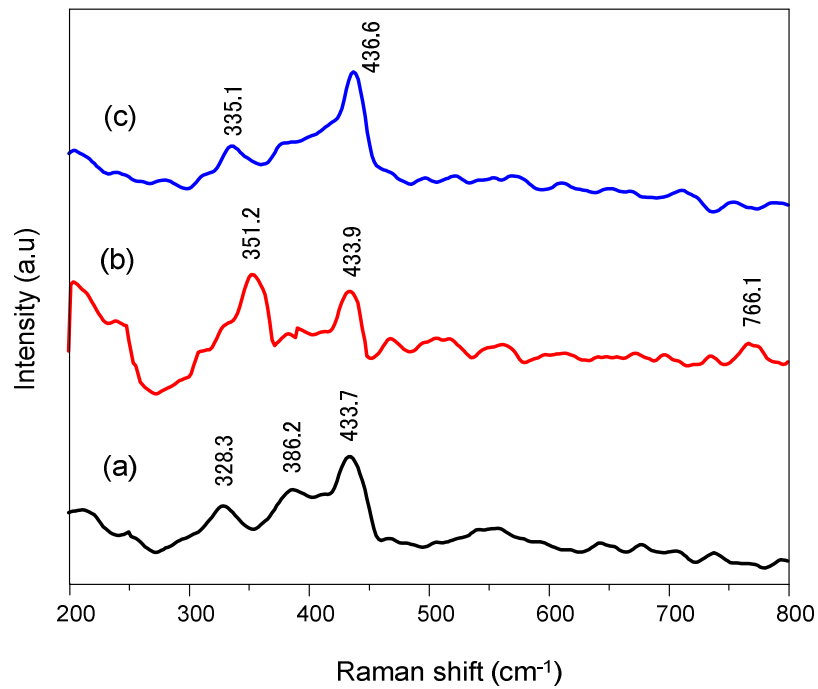


Figure 6: FT-Raman spectra of ZnO nanorods prepared using (a) CTAB (b) hydrazine hydrate and (c) solochemical method

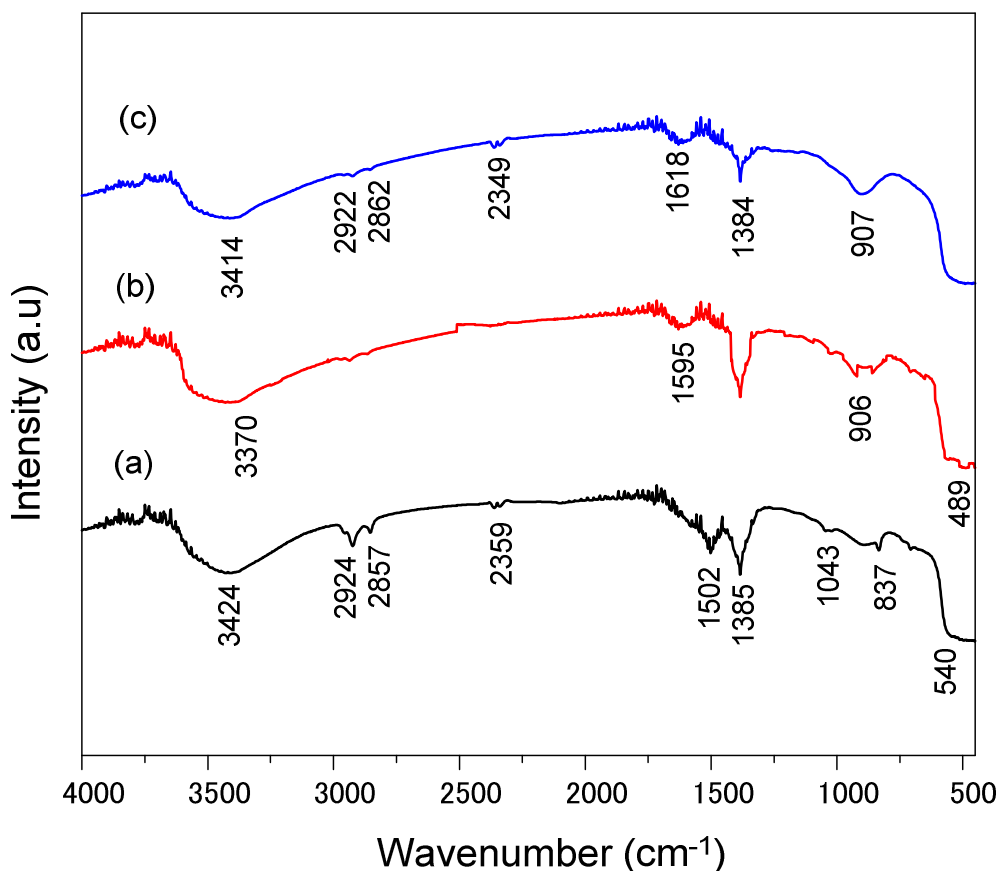


Figure 7: FT-IR spectra of ZnO nanorods prepared using (a) CTAB (b) hydrazine hydrate and (c) solochemical method

3.5 FT-Raman and FT-IR analysis

The room temperature Raman spectra of ZnO nanorods prepared via different growth conditions, with 1064 nm laser excitation are shown in Figure 6. The Raman active phonon modes at 433.7, 433.9 and 436.6 cm^{-1} are designated to E_2 (high) mode of ZnO. The other active Raman modes corresponding to E_2 (low), A_1 (TO), E_1 (TO), A_1 (LO) and E_1 (LO) are not visible. The FT-IR spectra of ZnO nanorod samples are depicted in Figure 7. The broad bands featured in the IR spectra of samples in the range between 3300 and 3400 cm^{-1} are assigned to O-H stretching mode vibrations. In Figure 7a, the peaks between 2800 and 3000 cm^{-1} may be due to C-H stretching vibration of residual CTA^+ species. The peak between 1500 and 1620 cm^{-1} corresponds to the scissoring mode of water molecule. The peaks positioned at 1385 and 1618 cm^{-1} are due to asymmetrical and symmetrical stretching of the zinc carboxylate originating from reactive carbon containing plasma species during synthesis [21]. The peaks at 490 and 540 cm^{-1} correspond to the stretching mode of ZnO.

3.6 TG-DTA studies

TGA was carried out to investigate the decomposition process of ZnO nanorod samples at elevated temperatures. As shown in Figure 8, the overall weight loss is between 0.5-3.5 % for all the three samples. The first step of the thermal decomposition is the loss of water molecules adsorbed at the surface at around 100 $^{\circ}\text{C}$, followed by the decomposition of $\text{Zn}(\text{OH})_2$ species at about 300-370 $^{\circ}\text{C}$ (Figure 8a, c). Whereas, in the case of the sample prepared with hydrazine hydrate (Figure 8b) the total weight loss is relatively less with 0.5 % which occurred at 500 $^{\circ}\text{C}$. It can be argued that ZnO prepared with hydrazine hydrate has high level of purity and contains lesser amount of hydroxyl species. The exothermic behaviour of the samples has been observed in DTA curves with the major intense peak between 220 and 250 $^{\circ}\text{C}$, indicating the thermal events that can be associated with the burning out of organic species (organic mass remained from CTAB) in the nanopowders. The energy released during the reaction is comparatively high for CTAB assisted sample when compared to hydrazine hydrate assisted and solochemically prepared samples. The two small exothermic peaks for the solochemical processed sample may be due to

decomposition of residual species, and that the absence of such secondary peaks for CTAB and hydrazine hydrate assisted samples again confirms the purity of ZnO products obtained.

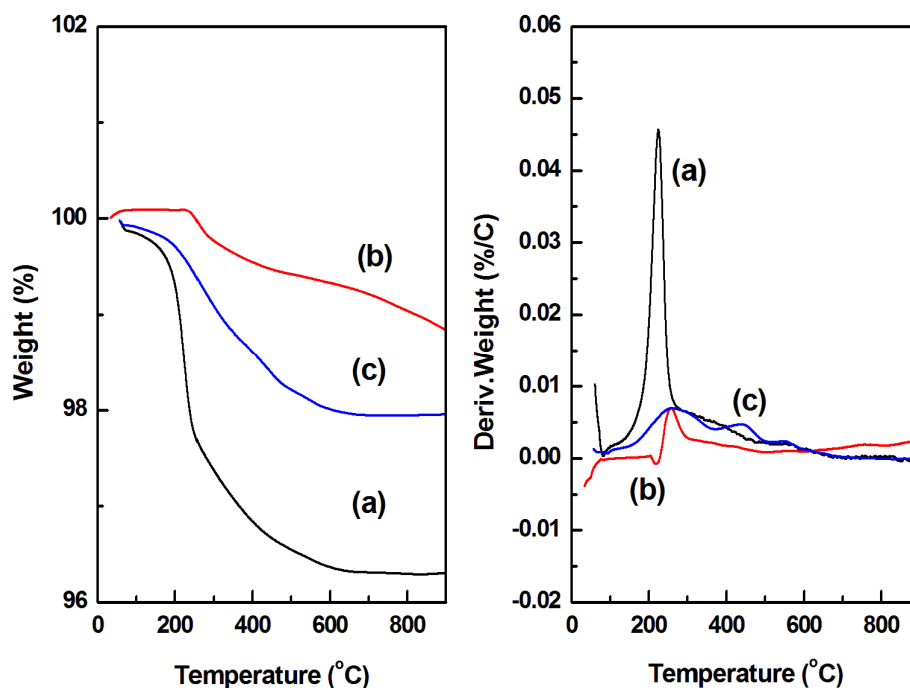


Figure 8: TG-DTA curves of ZnO nanorods prepared using (a) CTAB (b) hydrazine hydrate and (c) solochemical method

3.7 Microbial activity of ZnO

Antibacterial activity of the as-prepared rod-like nanostructures of ZnO was evaluated against inhibition zone area of Gram positive and negative bacteria. It is evident that there is a significant antibacterial activity (Figure 9) for ZnO nanorod samples over the three gram positive bacteria stains except *Bacillus subtilis* at room temperature. The mean zone of inhibition for ZnO against the microbes is ranged between 10 and 13 mm. The CTAB assisted and sonochemical processed crystallites exhibit higher mean zones of inhibition (13 mm) against Gram positive bacterium *Micrococcus lutes* than hydrazine hydrate. A moderate level of activity of about 12 and 11 mm is evident against *Staphylococcus epidermis* for those samples prepared using CTAB and solochemical approaches. The CTAB assisted ZnO exhibits less activity with 10 mm as zone of inhibition against *Staphylococcus aureus* and no anti-microbial activity was observed for sample prepared using hydrazine hydrate. Besides, no activity was found against gram negative bacteria for all the ZnO samples. It has been reported that the antimicrobial activity of ZnO superstructures is possibly due to the sufficiently reduced electron hole recombination rate at the surface interstitial defects [12]. Liu et al. have reported that ZnO superstructures leads to damage of cell walls due to the generation of highly reactive species such as H_2O_2 [22]. Since, oxide nanostructures are prone to surface defects and vacancies especially under low temperature conditions we believe that most of the defects on the surface of ZnO nanorod samples can be activated even under visible light. As a result electron-hole pairs can be created which could lead to the increased anti-microbial activity in the case of CTAB assisted ZnO and solochemical processed samples.

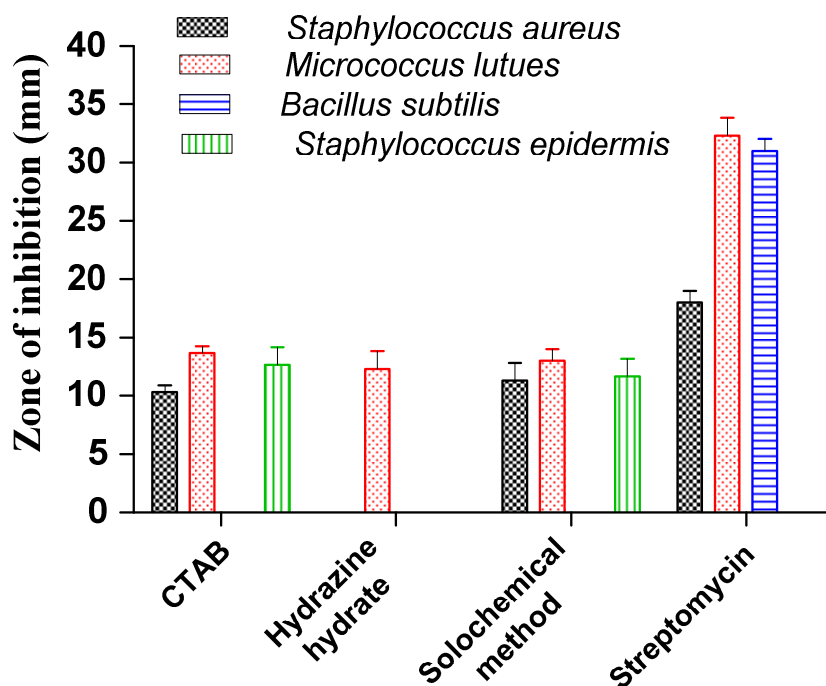


Figure 9: Measure of Zone of Inhibition as the antimicrobial activity of ZnO nanostructures

CONCLUSION

The ZnO nanostructures with distinct rod-like morphologies were successfully prepared using low temperature methods. The nanorods are size, shape controlled and highly dispersed that has been achieved with optimized temperature and time. The microscopic investigation concludes that obtained nanorods are phase pure, size reduced well below 50 nm in width and mostly agglomeration free. The overall minimum weight loss observed from the thermal investigation exhibit the phase purity of the nanorod. Significant antibacterial activity as the zone of inhibition over the gram positive bacteria stains were detected for ZnO rod-like nanostructures. Thus, low temperature solution based synthesis procedures with suitable surfactants and reducing agent can be employed to produce nanostructures of ZnO with high purity and homogeneity in size and shape.

Acknowledgement

The authors acknowledge Loyola College-Times of India (LC-TOI) Research initiative (Ref.No.3LCTOI14PHY001) for funding this research work and for providing the research facility at Department of Physics, Loyola College (Autonomous), Chennai -600034. We also thank Mr. Arul Maximus Rabel, Scientist, Centre for Nanoscience and Nanotechnology and Dr. Joseph Arul Pragasam, Professor of Physics, Sathyabama University for FESEM facility and for fruitful discussions.

REFERENCES

- [1] C. Y Jiang, X. W Sun, G. Q Lo, D. L Kwong, J. X Wang, *Applied Physics Letter*, **2007**, 90, 263501-263503.
- [2] A McLaren, T Valdes-Solis, G Li, S. C Tsang, *J. Am. Chem. Soc.* **2009**, 131, 12540-12541.
- [3] Qu Zhou, Weigen Chen, Lingna Xu and Shudi Peng, *Sensors*, **2013**, 13, 6171-6182.
- [4] C Jayaseelan, A Rahuman, A Vishnu Kirthi, S Marimuthu, T Santhoshkumar, A Bagavan, K Gaurav, L Karthik, K.V Bhaskara Rao, *Spectrochim. Acta Part A*, **2012**, 90, 78-84.
- [5] R Jalal, E. K Goharshadi, M Abareshi, M Moosavi, A Yousefi, P Nancarrow, *Mater. Chem. Phys.* **2010**, 121, 198-201.
- [6] M Huang, S Mao, H Feick, H Yan, Y Wu, H Kind, E Weber, R Russo, P Yang, *Science*, **2001**, 292, 1897-1899.
- [7] S. H Ko, D Lee, H. W Kang, K. H Nam, J. Y Yeo, S. J Hong, C. P Grigoropoulos, H. J Sung, *Nano Lett.* **2011**, 11, 666-671.

- [8] Y Qiu, K Yan, H Deng, S Yang, *Nano Lett.* **2012**, 12, 407–413.
- [9] J. X Wang, X. W Sun, Y Yang, H Huang, Y. C Lee, O. K Tan, L Vayssieres, *Nanotechnology*, **2006**, 292, 4995-4998.
- [10] E. S Jang, J. H Won, S. J Hwang and J. H Choy, *Adv. Mater.*, **2006**, 18, 3309–3312.
- [11] A McLaren, T Valdes-Solis, G Li, S. C Tsang, *J. Am. Chem. Soc.* **2009**, 131, 12540–12541.
- [12] T. R Lakshmeesha, M. K Sateesh, B Daruka Prasad, S. C Sharma, D Kavyashree, M Chandrasekhar, H Nagabhushana, *Cryst. Growth Des.*, **2014**, 14, 4068–4079.
- [13] M Premanathan, K Karthikeyan, K Jeyasubramanian, G Manivannan, *Nanotech. Biol. Med.* **2011**, 7, 184-192.
- [14] Lori E. Greene, Matt Law, Dawud H. Tan, Max Montano, Josh Goldberger, Gabor Somorjai, Peidong Yang, *Nano Lett.*, **2005**, 5, 1231–1236.
- [15] Yi Zeng, Tong Zhang, Lijie Wang, and Rui Wang, *J. Phys. Chem. C.*, **2009**, 113, 3442–3448.
- [16] Gusatti Marivone Campos, Carlos E. M Souza, Daniel A. R Kuhnen, Nivaldo C Riella, Humberto G Pizani, Paulo S, *J. Nanoscience and Nanotechnology*, **2012**, 12, 7986-7992.
- [17] Hui Zhang, Deren Yang, Yujie Ji , Xiangyang Ma , Jin Xu , and Duanlin Que, *J. Phys. Chem. B*, **2004**, 108, 3955–3958.
- [18] Yan-Xiang Wang, Jian Sun, XueYun Fan, Xi Yu, *Ceramics International* **2011**, 37, 3431-3436.
- [19] Hongliang Zhu, Deren Yang, and Hui Zhang, *Inorganic Materials*, **2006**, 42, 1210–1214.
- [20] Rohidas B. Kale, Shih-Yuan Lu, *Journal of Alloys and Compounds*, **2013**, 579, 444-449.
- [21] G Xiong, U Pal, J. G Serrano, K. B Ucer, R. T Williams, *Phys. stat. sol. (c)*, **2006**, 3, 3577–3581.
- [22] H. L Liu, T. C. K Yang, *Proc. Biochem.*, **2003**, 39, 475-481.